A NOVEL APPROACH TO THE DESIGN OF DUAL-BAND POWER DIVIDER WITH VARIABLE POWER DIVIDING RATIO BASED ON COUPLED-LINES

Z. Lin and Q.-X. Chu

School of Electronic and Information Engineering
South China University of Technology
Guangzhou, China

Abstract—This paper presents an approach to the design of a novel dual-band power divider with variable power dividing ratio. To achieve dual-band operation, a novel dual-band quarter-wave length transformer based on coupled-lines is proposed, which is used to replace the quarter-wave length transformer in Wilkinson power divider. The proposed dual-band power divider features a simple compact planar structure with wide bandwidth performance for small frequency ratio. Closed-form design equations with one degree of design freedom are derived using even- and odd-mode analysis and transmission line theory. For verification purpose, power dividers operating at 2.4/3.8 GHz with dividing ratios of 2 : 1 and 1 : 1 are designed, simulated and measured. The simulated and measured results are in good agreement.

1. INTRODUCTION

Recently, rapid developments in modern wireless communication industry have imposed their radio frequency (RF) components to operate at multiple frequency bands. Many efforts have been made to develop more versatile dual-band components such as antennas [1–4], filters [5–8], coupler [9, 10] and transformers [11, 12]. Meanwhile, the power divider as one of the most important passive circuits has been widely used in microwave and communication systems. It is crucial to design dual-band power dividers for practical applications. In the past, several approaches were proposed for the design of dual-band power divider [13–28]. In [13], a power divider using two-section transmission lines cascaded was introduced with the main drawback of

---

Corresponding author: Q.-X. Chu (qxchu@scut.edu.cn).

poor isolation and output return loss. Some improved topologies [14–16] were proposed by adding parallel RLC [14, 15] and combining series and parallel RLC [16], which may result in parasitic effect especially at high frequency. A dual-band topology based on stepped impedance [17] was presented, but the major shortfalls of this scheme are poor isolation and output return loss. Some designs by adding shunt stubs [18–20] were recommended, but they have defect of large size [18, 19] or poor bandwidth [20]. Another design using extended ports [21, 22] was introduced, which is inconvenient for design because of falling short of closed-form design formulas. An improved variation is present in [23], which employed a coupled-line section at the output and eliminated the need of the input port extension. Artificial transmission lines were also used to realize dual-band operation [24]. But all of the above dual-band power dividers [13–24] were all equal power dividing structures. In order to achieve variable power dividing ratio, some topologies [25–28] were proposed. But the employ of lumped reactance elements may cause parasitic effect [25, 26]. And also the design in [26] only can be applied in the dual-band systems whose frequency ratio is equal to 2. An improved structure without reactive components was proposed in [27]. Another dual-band unequal divider based on T-type transformer was designed but it suffered from poor output matching and isolation [28].

In this paper, a novel dual-band quarter-wave length transformer based on coupled-lines is proposed and analyzed firstly. Then by substituting the proposed dual-band transformer for the quarter-wave length transmission line in conventional Wilkinson power divider, a novel dual-band power divider with variable power dividing ratio is proposed and analyzed. The proposed structure features a simple distribution structure (without any lumped reactive component) with wide bandwidth performance for small frequency ratio, ideal return loss and port isolation and closed-form design formulas with one degree of design freedom. In fact, the following analysis and design method can be regarded as the generalization of the dual-band power divider with variable power dividing ratio.

2. THEORETICAL ANALYSIS

The circuit construction of the proposed dual band power divider is shown in Figure 1. In order to make the analysis of this proposed structure simple and convenient, the method of using dual-band elements to replace single-band ones will be applied. The conventional Wilkinson power divider with variable dividing ratio [29], as shown in Figure 2, will be recalled firstly. Then a novel dual-band transformer
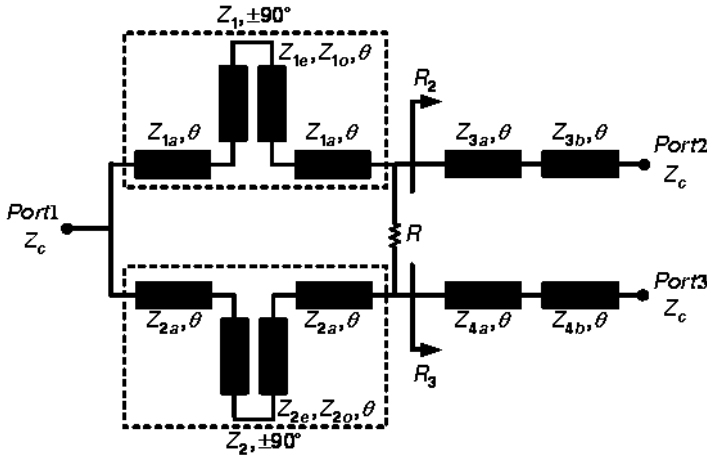
Figure 1. Proposed structure of dual-band power divider.

will be proposed and analyzed. Subsequently the single-band elements (Z_1, Z_2, T_3 and T_4) will be replaced by dual-band structures to accomplish dual-band function. Assume that the ratio of the output power at ports 3 and 2 is equal to $k^2 (= P_3/P_2)$ in the following analysis.

2.1. Conventional Wilkinson Power Divider

As shown in Figure 2, the following resistance relationships must be satisfied to accomplish variable dividing ratio in conventional Wilkinson power divider [29]:

$$R_2 = Z_c k \tag{1}$$

$$R_3 = Z_c/k \tag{2}$$

$$R = Z_c \left(k + \frac{1}{k} \right) \tag{3}$$

$$Z_1 = Z_c \sqrt{k(1 + k^2)} \tag{4}$$

$$Z_2 = Z_c \sqrt{\frac{(1 + k^2)}{k^3}}. \tag{5}$$

Note that the output lines are matched to the impedances R_2 and R_3, which are not matched to the ports impedance Z_c. Matching transformers T_3 and T_4 can be employed to transform these output impedances. It can be observed that the results reduce to the equal dividing case for $k = 1$.
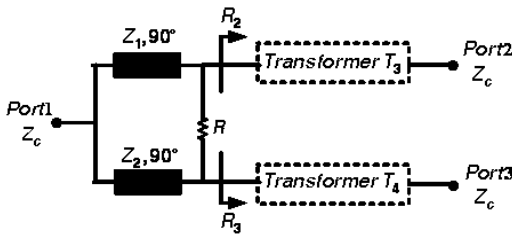
(a)

(b)

Figure 2. Conventional Wilkinson power divider with variable dividing ratio.
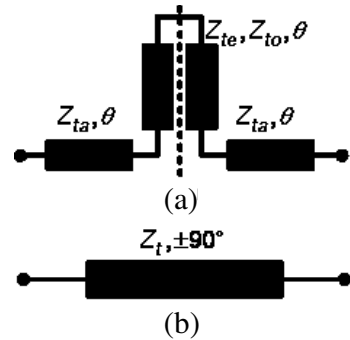
Figure 3. (a) Proposed dual-band quarter-wave length transformer. (b) Equivalent structure.

2.2. Dual-band Elements

Two kinds of elements, as shown in Figure 2, should be replaced by dual-band structures. One is quarter-wave length transmission line (Z_1 and Z_2), and the other is output transformer (T_3 and T_4) with no electrical length requirement. The novel dual-band quarter-wave length transformer based on coupled-lines, as shown in Figure 3, is proposed to replace the first kind of element, while the two-section dual-band transformer [30] is used to replace the second kind of element.

Figure 3(a) shows the proposed dual-band quarter-wave length transformer, which consists of parallel coupled-lines with even impedance of Z_{te}, odd impedance of Z_{to} and electrical length of θ, connected to a pair of branch-line with characteristic impedance Z_{ta} and electrical length of θ. In the above symbols, variable $t = 1, 2$. This proposed structure is equivalent to a quarter-wave length transmission line with characteristic impedance of Z_t and electrical length of $\pm 90°$, as illustrated in Figure 3(b). Suppose when the proposed transformer operates at f_1 and f_2, the electrical length of the equivalent circuit is $+90°$ and $-90°$, respectively. For the sake of analysis, the proposed structure is assumed to be lossless and reciprocal. The dual-band quarter-wave length transformer is symmetric and the circuit parameters, therefore, can be determined using the even- and odd-mode analysis.

As depicted in Figure 4, the proposed even half-circuit equals an open-ended stub with characteristic impedance of Z_t and electrical
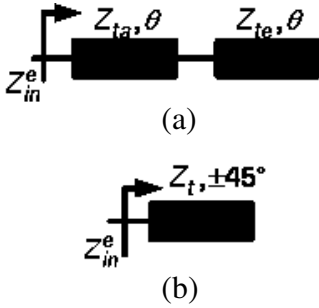
Figure 4.   Even half-circuit. (a) Proposed dual-band quarter-wave length transformer.   (b) Equivalent structure.
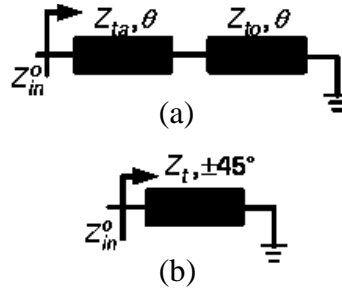

Figure 5.   Odd half-circuit. (a) Proposed dual-band quarter-wave length transformer.   (b) Equivalent structure.

length of $\pm 45°$. As shown in Figure 4(a), the input impedance of the proposed even half-circuit is equal to

$$Z_{in}^e = jZ_{ta}\frac{-Z_{te} + Z_{ta}\tan^2\theta}{(Z_{ta} + Z_{te})\tan\theta}. \tag{6}$$

From Figure 4(b), the input impedance of the open-ended stub is equal to

$$Z_{in}^e = -jZ_t\cot(\pm 45°). \tag{7}$$

By combining (6) and (7), the equivalent impedance of Z_t can be written as

$$Z_t = Z_{ta}\frac{Z_{te} - Z_{ta}\tan^2\theta}{\pm\tan\theta(Z_{ta} + Z_{te})}, \tag{8}$$

As shown in Figure 5, the proposed odd half-circuit is equal to a short-ended stub with characteristic impedance of Z_t and electrical length of $\pm 45°$. As shown in Figure 5(a), the input impedance of proposed odd half-circuit is equal to

$$Z_{in}^o = jZ_{ta}\frac{(Z_{to} + Z_{ta})\tan\theta}{Z_{ta} - Z_{to}(\tan\theta)^2}. \tag{9}$$

From Figure 5(b), the input impedance of the short-ended stub is equal to

$$Z_{in}^o = jZ_t\tan(\pm 45°). \tag{10}$$

By combining (9) and (10), the equivalent impedance of Z_t can be written as

$$Z_t = Z_{ta}\frac{\pm\tan\theta(Z_{ta} + Z_{to})}{Z_{ta} - Z_{to}\tan^2\theta}. \tag{11}$$

From (8) or (11), for dual-band operation, the necessary condition may simply be stated as

$$\tan \theta_1 = -\tan \theta_2. \tag{12}$$

where θ_1 and θ_2 are electrical lengths of coupled-lines or branch-lines evaluated at the frequencies of f_1 and f_2.

The general solution of (12) can then be expressed as

$$\theta_1 + \theta_2 = p\pi \tag{13}$$

where $p = 1, 2, 3, \ldots$, and taking into account that

$$\frac{\theta_2}{\theta_1} = \frac{f_2}{f_1}, \tag{14}$$

one obtains

$$\sigma = \frac{\frac{f_2}{f_1} - 1}{\frac{f_2}{f_1} + 1} \tag{15}$$

$$f_0 = \frac{f_1 + f_2}{2} \tag{16}$$

$$\theta_1 = \frac{p\pi}{2} \cdot \frac{f_1}{f_0} = \frac{p\pi}{2}(1 - \sigma) \tag{17}$$

$$\theta_2 = \frac{p\pi}{2} \cdot \frac{f_2}{f_0} = \frac{p\pi}{2}(1 + \sigma). \tag{18}$$

It is observed that the electrical length of the coupled-lines or branch-line can be evaluated at f_0 as

$$\theta_0 = \frac{\theta_1 + \theta_2}{2} = \frac{p\pi}{2}. \tag{19}$$

Subsequently, based on (8), (11) and (17) or (18) can be rewritten as

$$Z_{te} = Z_{ta} \frac{Z_{ta} \cot^2(\theta_0 \pi) + Z_t \cot(\theta_0 \pi)}{Z_{ta} - Z_t \cot(\theta_0 \pi)} \tag{20}$$

$$Z_{to} = Z_{ta} \frac{Z_t - Z_{ta} \cot(\theta_0 \pi)}{Z_t \cot^2(\theta_0 \pi) + Z_{ta} \cot(\theta_0 \pi)} \tag{21}$$

for $p = 1, 3, 5 \ldots$, and

$$Z_{te} = Z_{ta} \frac{Z_{ta} \tan^2(\theta_0 \pi) - Z_t \tan(\theta_0 \pi)}{Z_{ta} + Z_t \tan(\theta_0 \pi)} \tag{22}$$

$$Z_{to} = Z_{ta} \frac{Z_t + Z_{ta} \tan(\theta_0 \pi)}{Z_t \tan^2(\theta_0 \pi) - Z_{ta} \tan(\theta_0 \pi)} \tag{23}$$

for $p = 2, 4, 6 \ldots$.

In referring to Equations (20)–(23), there are two degrees of design freedom in choosing variable p and the characteristic impedance of Z_{ta} of the branch-line, which means infinite solutions for the design and makes the design more flexible. However, for the purpose of compact size, only $p = 1$ is chosen and discussed in this paper. There is one degree of design freedom left when the value of p is decided. Figure 6 shows the circuit parameters (even mode impedance of Z_{te} and odd mode impedance of Z_{to} of the coupled-lines) calculated as a function of frequency ratio (f_1/f_2) when Z_{ta} and Z_t are $50\,\Omega$ and $70.71\,\Omega$ respectively. It is then observed that the proposed dual-band power divider can operate over a range of small frequency ratio $(f_2/f_1 < 1.64)$.

In order to achieve output ports matching at both required frequencies, a two-section dual-band transformer based on Monzon's theory [30] is employed to replace the output transformer in conventional Wilkinson power divider. The characteristic impedances of output transformers connected to ports 2 and 3, as shown in Figure 1, can be determined by

$$\alpha = \tan(\theta_1)^2 \tag{24}$$

$$t_n = R_n/Z_c \tag{25}$$

$$Z_{na} = Z_c\sqrt{\frac{t_n}{2\alpha}(1 - t_n) + \sqrt{\left[\frac{t_n}{2\alpha}(1 - t_n)\right]^2 + k^3}} \tag{26}$$

$$Z_{nb} = R_2 Z_c/Z_{na} \tag{27}$$

where the definition of θ_1 is same to (17), and $n = 3, 4$.

2.3. Dual-band Power Divider

So far, all design equations have been derived. With all symbols referring to Figure 1, the design procedure can be summarized as follows:

1) According required power dividing ratio k^2, use (1)and (2) to compute the output impedance, (3) to get the isolation resistor value, (4) and (5) to calculate equivalent quarter-wave length line impedance of Z_1 and Z_2.

2) Use (19) to compute the electrical length θ for all branch-lines. After choosing realizable values for Z_{1a} and Z_{2a}, use (20) and (21) to get Z_{1e}, Z_{1o}, Z_{2e} and Z_{2o}.

3) Use (26) and (27) to get the characteristic impedances of output transformers of Z_{3a}, Z_{3b}, Z_{4a} and Z_{4b}.
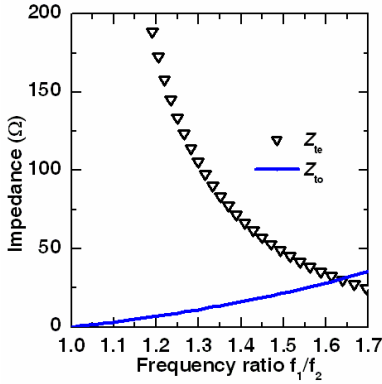
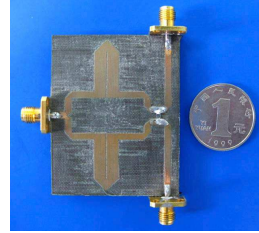**Figure 6.** Circuit parameters versus frequency ratio.

Figure 7. Photograph of the designed equal dual-band power divider.

3. SIMULATED AND MEASURED RESULTS

In this section, two dual-band power dividers operating at Wimax 2.4/3.8 GHz have been designed, simulated and fabricated to verify the proposed design method. The electromagnetic simulator Zeland IE3D were employed to tune the layout and the scattering parameter measurements were performed using an Agilent N5230A network analyzer over the frequency from 1.5 to 4.5 GHz. When using IE3D to tune the proposed structures, it often doesn't need to tune the width of microstrip lines, while the length of which just need fine-tuning. And the microstrip discontinuity should be carefully tuned based on the technique of mitering [29]. Zeland LineGauge is used to obtain initial dimensions. Both two power dividers were fabricated on a 0.8-mm-thick substrate with a relative permittivity of 2.55. The port impedances are 50 Ω.

3.1. Equal Dual-Band Power Divider

According to the design procedure in Section 2, an equal dual-band power divider i.e. power dividing ratio $k^2 = 1$ is designed. After choosing branch-line impedances of Z_{1a} and Z_{2a} both as 50 Ω, θ_0 is calculated as $\Pi/2$. The design parameters are shown in Table 1.

Figure 7 shows the photograph of the designed equal dual-band power divider. Figure 8 shows the comparison of simulated and measured results which are in good agreement. Figure 8(a) shows that the transmission ($|S_{21}|$ and $|S_{31}|$) are both better than -3.6 dB, and their magnitudes are almost the same, which denotes that the signal is almost equally divided into two output ports both at 2.4

Table 1. Design parameters of equal power divider.

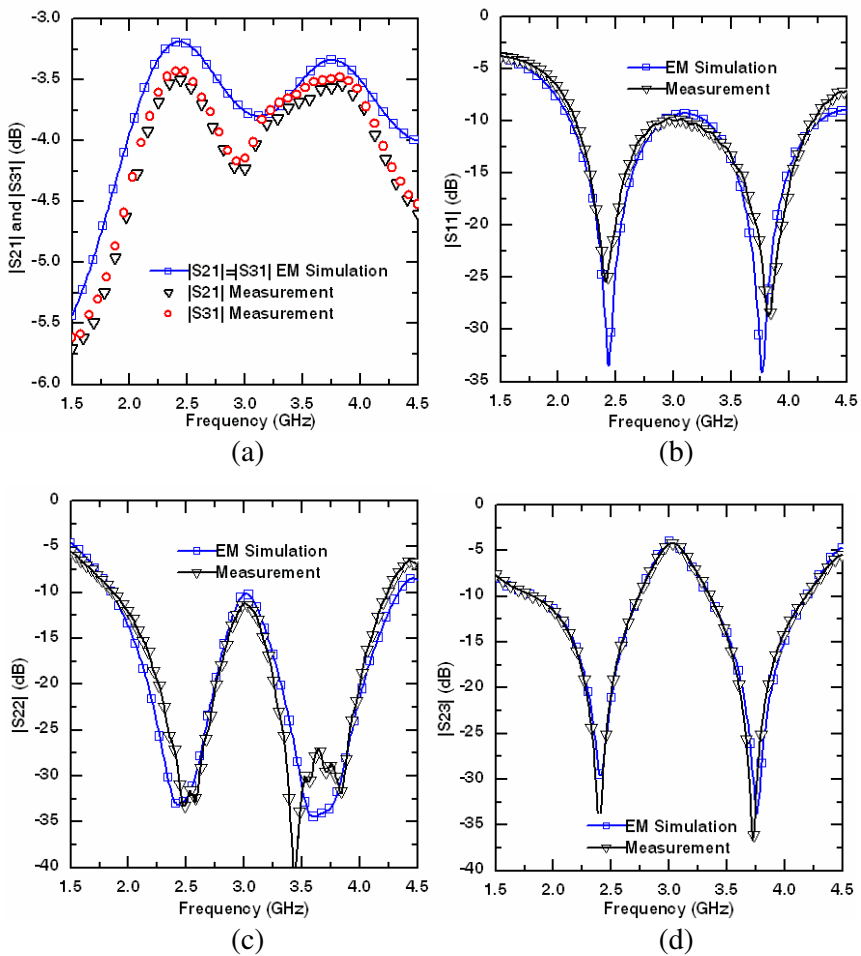|	Coupled-lines			Branch lines		Output transformers	
Electrical parameters	$Z_{1e} = Z_{2e}$		$Z_{1o} = Z_{2o}$	$Z_{1a} = Z_{2a}$		$Z_{3a} = Z_{3b} = Z_{4a} = Z_{4b}$	
Impedance (Ω)	36.1		27.0	50		50	
Physical parameters	Width	Space	Length	Width	Length	Width	Length
Initial values (mm)	4.1	0.3	16.5	2.2	16.5	2.2	16.5
Final values (mm)	4.1	0.3	16.8	2.2	16.9	2.2	16.5

Figure 8. Simulated and measured results of equal dual-band power divider. (a) Transmission ($|S_{21}|$ and $|S_{31}|$). (b) Input matching ($|S_{11}|$). (c) Output matching ($|S_{22}| = |S_{33}|$). (d) Isolation ($|S_{23}|$).

and 3.8 GHz. Figures 8(b) and (c) indicate that the input ($|S_{11}|$) and output matching ($|S_{22}|$) are well below -25 dB. And a good isolation ($|S_{23}| < -30$ dB) is also achieved as shown in Figure 8(d). The proposed structure shows good bandwidth performance at dual-band operation. With $|S_{11}|$, $|S_{22}|$ and $|S_{23}|$ all below -20 dB, and the measured bandwidth of lower band is found to be about 178 MHz approximately, while that of upper band is about 230 MHz.

3.2. Unequal Dual-band Power Divider

According to the design procedure in Section 2, an unequal dual-band power divider with power dividing ratio $k^2 = 2$ are designed. After choosing branch-line impedances of Z_{1a} and Z_{2a} as $75\,\Omega$ and $52\,\Omega$, respectively, the design values are computed as follows: $\theta_0 = \Pi/2$, $R = 106.06\,\Omega$, $Z_{1e} = 56.35\,\Omega$, $Z_{1o} = 42.20\,\Omega$, $Z_{2e} = 64.66\,\Omega$, $Z_{2o} = 42.92\,\Omega$, $Z_{3a} = 64.06\,\Omega$, $Z_{3b} = 55.19\,\Omega$, $Z_{4a} = 39.02\,\Omega$, $Z_{4b} = 45.30\,\Omega$.

Figure 9 shows the photograph of the unequal dual-band power divider. Figure 10 show the comparison of simulated and measured results which are in good agreement. Figure 10(a) shows that the measured $|S_{21}|$ are -5.14 dB at 2.4 GHz and -5.22 dB at 3.8 GHz, while $|S_{31}|$ are -2.09 at 2.4 GHz and -2.40 dB at 3.8 GHz. Thereby, the power dividing ratio is 3.05 dB at 2.4 GHz and 2.82 dB at 3.8 GHz, which are very close to the theoretical value of 3 dB. From Figure 10(b), the input matching of $|S_{11}|$ are below -26 dB at both 2.4 GHz and 3.8 GHz. The output matching of $|S_{22}|$ and $|S_{33}|$ are given in Figure 10(c), which shows that both $|S_{22}|$ and $|S_{33}|$ are below -24 dB at both 2.4 GHz and 3.8 GHz. The isolation performance of $|S_{23}|$ can be observed in Figure 10(d), which shows that the $|S_{23}|$ are below -29 dB at both 2.4 GHz and 3.8 GHz. With $|S_{11}|$, $|S_{22}|$, $|S_{33}|$ and $|S_{23}|$ all below -20 dB, the measured bandwidth of lower band is found to be about 209 MHz approximately, while that of upper band is about 210 MHz. For comparison, the structure [27] which do not need any lumped reactance elements and could operate at the same frequency (2.4/3.8 GHz) with power dividing ratio ($k^2 = 2$) has been simulated. With $|S_{11}|$, $|S_{22}|$, $|S_{33}|$ and $|S_{23}|$ all below -20 dB, the simulated bandwidth of lower band is found to be 101 MHz approximately, while that of upper band is about 82 MHz. It can be easily found that the bandwidth of the proposed structure is more than 2 times wider than that of [27], which means the significant wide bandwidth contribution from the proposed design.
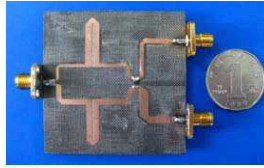
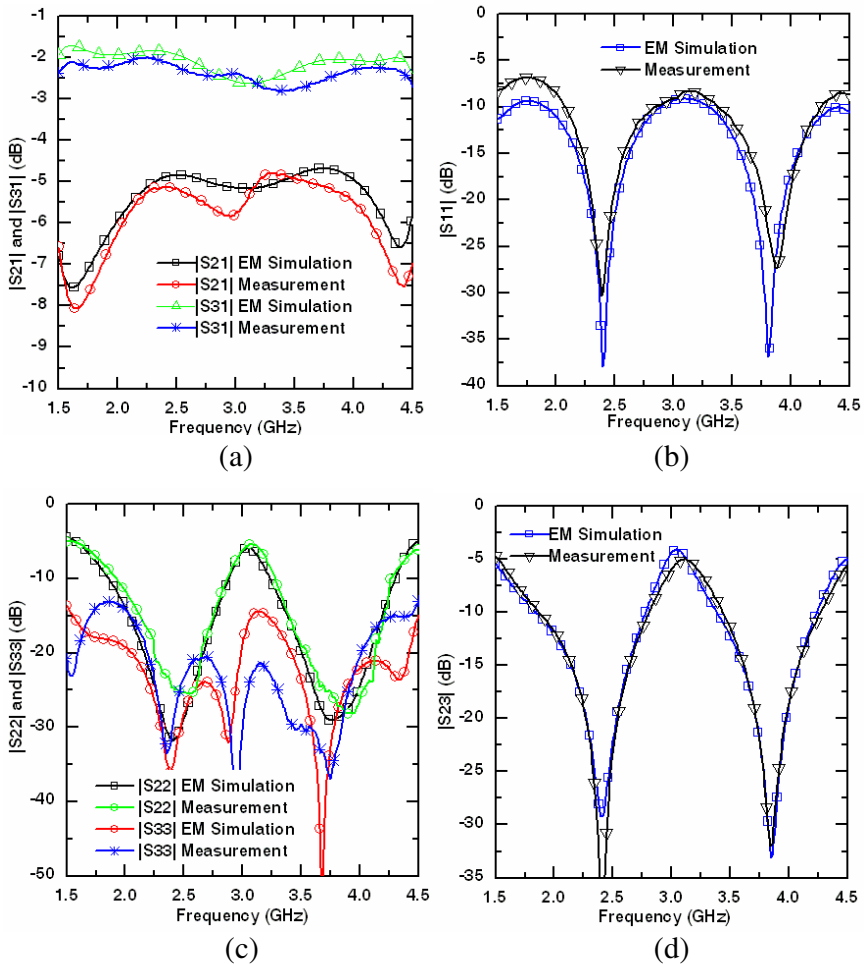**Figure 9.** hotograph of the designed unequal dual-band power divider.

Figure 10. Simulated and measured results of unequal dual-band power divider. (a) Transmission ($|S_{21}|$ and $|S_{31}|$). (b) Input matching ($|S_{11}|$). (c) Output matching ($|S_{22}|$ and $|S_{33}|$). (d) Isolation ($|S_{23}|$).

4. CONCLUSION

An approach to the design of novel dual-band power divider with variable power dividing ratio using coupled-lines has been presented. Applying even- and odd-mode analysis and transmission line theory, closed-form design formulas have been derived. For verification, two experimental prototypes have been designed, simulated and fabricated. Good agreement between the simulated and measured results has been observed, which demonstrates that the proposed circuit fulfills variable power dividing ratio, wide bandwidth for small band ratio, equal power split, good isolation and well impedance matching.

ACKNOWLEDGMENT

REFERENCES

1. Xiong, J.-P., L. Liu, X.-M. Wang, J. Chen, and Y.-L. Zhao, "Dual-band printed bent slots antenna for WLAN applications," *Journal of Electromagnetic Waves and Applications*, Vol. 22, No. 11–12, 1509–1515, 2008.

2. Ren, W., "Compact dual-band slot antenna for 2.4/5 GHz WLAN applications," *Progress In Electromagnetics Research B*, Vol. 8, 319–327, 2008.

3. Anguera, J., C. Puente, and C. Borja, "Dual frequency broadband microstrip antenna with a reactive loading and stacked elements," *Progress In Electromagnetics Research Letters*, Vol. 10, 1–10, 2009.

4. Behera, S. and K. J. Vinoy, "Microstrip square ring antenna for dual-band operation," *Progress In Electromagnetics Research*, PIER 93, 41–56, 2009.

5. Alkanhal, M. A. S., "Dual-band bandpass filters using inverted stepped-impedance resonators," *Journal of Electromagnetic Waves and Applications*, Vol. 23, No. 8–9, 1211–1220, 2009.

6. Fallahzadeh, S., H. Bahrami, and M. Tayarani, "A novel dual-band bandstop waveguide filter using split ring resonators," *Progress In Electromagnetics Research Letters*, Vol. 12, 133–139, 2009.

7. Lin, W.-J., C.-S. Chang, J.-Y. Li, D.-B. Lin, L.-S. Chen, and M.-P. Houng, "A new approach of dual-band filters by stepped

impedance simplified cascaded quadruplet resonators with slot coupling," *Progress In Electromagnetics Research Letters*, Vol. 9, 19–28, 2009.

8. Velazquez-Ahumada, M. D. C., J. Martel-Villagr, F. Medina, and F. Mesa, "Application of stub loaded folded stepped impedance resonators to dual band filters," *Progress In Electromagnetics Research*, PIER 102, 107–124, 2010.

9. He, J., B.-Z. Wang, and K.-H. Zhang, "Arbitrary dual-band coupler using accurate model of composite right/left handed transmission line," *Journal of Electromagnetic Waves and Applications*, Vol. 22, No. 8–9, 1267–1272, 2008.

10. De Castro-Galan, D., L. E. Garcia Munoz, D. Segovia-Vargas, and V. Gonzalez-Posadas, "Diversity monopulse antenna based on a dual-frequency and dual mode CRLH rat-race coupler," *Progress In Electromagnetics Research B*, Vol. 14, 87–106, 2009.

11. Wu, Y., Y. Liu, and S. Li, "A compact Pi-structure dual band transformer," *Progress In Electromagnetics Research*, PIER 88, 121–134, 2008.

12. Castaldi, G., V. Fiumara, and I. Gallina, "An exact synthesis method for dual-band Chebyshev impedance transformers," *Progress In Electromagnetics Research*, PIER 86, 305–319, 2008.

13. Srisathit, S., M. Chongcheawchamnan, and A. Worapishet, "Design and realization of dual-band 3 dB power divider based on two-section transmission-line topology," *IET Electronics Letters*, Vol. 39, No. 9, 723–724, May 1, 2003.

14. Wu, L., H. Yilmaz, T. Bitzer, A. Pascht, and M. Berroth, "A dual-frequency Wilkinson power divider: For a frequency and its first harmonic," *IEEE Microw. Wireless Compon. Lett.*, Vol. 15, No. 2, 107–109, Feb. 2005.

15. Wu, L., S. Sun, H. Yilmaz, and M. Berroth, "A dual-frequency Wilkinson power divider," *IEEE Trans. Microw. Theory Tech.*, Vol. 54, No. 1, 278–284, Jan. 2006.

16. Wu, Y., Y. Liu, and S. Li, "A new dual-frquency Wilkinson power divider," *Journal of Electromagnetic Waves and Applications*, Vol. 23, No. 4, 483–492, 2009.

17. Avrillon, S., I. Pele, A. Chousseaud, and S. Toutain, "Dual-band power divider based on semiloop stepped-impedance resonators," *IEEE Trans. Microw. Theory Tech.*, Vol. 51, No. 4, 1269–1273, Apr. 2003.

18. Cheng, K.-K. M. and F.-L. Wong, "A new Wilkinson power divider design for dual band applications," *IEEE Microw. Wireless*

Compon. Lett., Vol. 17, No. 9, 664–666, Sep. 2007.

19. Zhang, H. and H. Xin, "Designs of dual-band Wilkinson power dividers with flexible frequency ratios," *IEEE MTT-S Int. Microw. Symp. Dig.*, 1223–1226, 2008.

20. Cheng, K.-K. M. and C. Law, "A novel approach to the design and implementation of dual-band power divider," *IEEE Trans. Microw. Theory Tech.*, Vol. 54, No. 2, 487–492, Feb. 2008.

21. Park, M.-J. and B. Lee, "Wilkinson power divider with extended ports for dual-band operation," *IET Electronics Letters*, Vol. 44, No. 15, 916–917, Jul. 17, 2008.

22. Li, X., S.-X. Gong, L. Yang, and Y.-J. Yang, "A novel Wilkinson power divider for dual-band operation," *Journal of Electromagnetic Waves and Applications*, Vol. 23, No. 2–3, 395–404, 2009.

23. Park, M.-J., "Dual-band wilkinson divider with coupled output port extensions," *IEEE Trans. Microw. Theory Tech.*, Vol. 57, No. 9, 2232–2237, 2009.

24. Yang, T., C. Liu, L. Yan, and K. Huang, "A compact dual-band power divider using planar artificial transmission lines for GSM/DCS applications," *Progress In Electromagnetics Research Letters*, Vol. 10, 185–191, 2009.

25. Wu, Y., Y. Liu, and S. Li, "An unequal dual-frequency Wilkinson power divider with optional isolation structure," *Progress In Electromagnetics Research*, PIER 91, 393–411, 2009.

26. Wu, Y., H. Zhou, Y. Zhang, and Y. Liu, "An unequal Wilkinson power divider for a frequency and its first harmonic," *IEEE Microw. Wireless Compon. Lett.*, Vol. 18, No. 11, 737–739, Sep. 2008.

27. Wu, Y., Y. Liu, Y. Zhang, J. Gao, and H. Zhou, "A dual band unequal Wilkinson power divider without reactive components," *IEEE Trans. Microw. Theory Tech.*, Vol. 57, No. 1, 216–222, 2009.

28. Li, X., Y. -J. Yang, L. Yang, S.-X. Gong, X. Tao, Y. Gao, K. Ma, and X.-L. Liu, "A novel design of dual-band unequal Wilkinson power divider," *Progress In Electromagnetics Research C*, Vol. 12, 93–100, 2010.

29. Pozar, D., *Microwave Engineering*, 3rd edition, Wiley, New York, 2005.

30. Monzon, C., "A small dual-frequency transformer in two section," *IEEE Trans. Microw. Theory Tech.*, Vol. 51, No. 4, 1157–1161, Apr. 2003.